



A Mathematical Model of Vascular Tumour Growth and Invasion

M. E. ORME AND M. A. J. CHAPLAIN

School of Mathematical Sciences, University of Bath

Bath BA2 7AY, United Kingdom

<meo><majc>@maths.bath.ac.uk

(Received and accepted August 1995)

Abstract—In this paper, we develop a simple mathematical model of the vascularization and subsequent growth of a solid spherical tumour. The key elements that are encapsulated in this model are the development of a central necrotic core due to the collapse of blood vessels at the centre of the tumour and a peak of tumour cells advancing towards the main blood vessels together with the regression of newly-formed capillaries. Diffusion alone cannot account for all observed behaviour, and hence, we include ‘taxis’ in our model, whereby the movement of the tumour cells is directed towards high blood vessel densities. This means that the growth of the tumour is accompanied by the invasion of the surrounding tissue. Invasion is closely linked to metastasis, whereby tumour cells enter the blood or lymph system and hence secondary tumours or metastases may arise. In the second part of the paper, we conduct a travelling wave analysis on a simplified version of the model and obtain bounds on the parameters such that the solutions are nonnegative and hence biologically relevant and also an estimate for the rate of invasion.

Keywords—Vascularization, Tumour growth, Invasion.

1. INTRODUCTION

Perhaps the most important feature that distinguishes a malignant tumour from a benign tumour is its ability to invade surrounding tissue. Invasion is often followed by metastasis, whereby tumour cells are spread via the blood or the lymph system to other parts of the body where they may form distant colonies (metastases). This results in multiple secondary tumours [1], and hence, the disease cannot be cured by treating the original tumour alone, thus making any attempt at treatment very difficult as eradication of the secondary tumours often leads to damage of the normal tissue.

The onset of metastasis is necessarily preceded by the vascularization of a solid tumour nodule (e.g., carcinoma) by a process known as angiogenesis. Initially the tumour is avascular; i.e., it does not have its own blood supply. The tumour is very small at this stage (1–3 mm in diameter) and takes in nutrients and expels waste products by diffusion mechanisms alone. However, this mechanism limits the growth of the tumour [2,3]. As the tumour grows, demand increases and nutrients diffusing through the surface of the tumour are used up before they can reach the centre. Cells at the middle of the tumour are starved of nutrients and begin to die [4]. A necrotic core will develop and eventually there will be an equilibrium between the necrotic cells at the centre and the outer layer of proliferating cells. The tumour will become dormant and growth will stop.

The tumour can overcome this deficiency by acquiring a blood supply and it does so by inducing any neighbouring blood vessels to grow towards the tumour [5,6]. The formation of blood vessels is called angiogenesis. Angiogenesis is not unique to tumour growth, and it is also ev-

Typeset by $\mathcal{A}\mathcal{M}\mathcal{S}\text{-}\mathcal{T}\mathcal{E}\mathcal{X}$

ident in many other pathological conditions such as diabetic retinopathy, arthritis and chronic inflammation [7,8]. Tumour angiogenesis is initiated by the release of certain chemicals known as tumour angiogenesis factors, or TAF, by the tumour [9]. This stimulates the endothelial cells (EC) in neighbouring blood vessels to migrate towards the tumour. Capillary sprouts are formed which grow in length by recruiting EC from the parent vessel [10]. Neighbouring sprouts will eventually fuse together at their tips to form loops (anastomoses). The looped vessels themselves may bud or may fuse with other loops until a complex network of vessels develop. This network will eventually penetrate the tumour and furnish it with the nutrients it requires for continued growth.

A vascularized tumour, that is, a tumour which is permeated with blood vessels, rapidly increases in mass. This enormous growth in tumour volume results in the collapse of the vasculature at the centre of the tumour and once again a necrotic core will develop surrounded by a peripheral zone of live cells or 'tumour vascular envelope' [8]. In order to support continued growth, the tumour's vascular system persistently remodels itself, continuing indefinitely until the tumour is removed or killed, or until the host dies. Hence, it is desirable to prevent a tumour from reaching the vascular phase of growth. The inhibition of angiogenesis may lead to the inhibition of tumour growth [4,11-13]

In the following section, we will derive a simple minimal mathematical model which describes the interaction between the cells of the growing tumour mass and its vasculature. We present some numerical simulations which show this interaction for different initial conditions. In Section 3, the model is slightly modified and we look for travelling wave solutions with constant speed and profile. Finally, in Section 4, we make various concluding remarks.

2. THE MATHEMATICAL MODEL

This model examines the development of the tumour vascular envelope from the onset of vascularization to the eventual invasion of the (parent) blood vessel, which may consequently lead to metastasis. We assume that the tumour has successfully induced angiogenesis; that is, a network of capillary vessels has just reached the tumour boundary. We do not explicitly model the concentration of TAF, though this is incorporated into the model by presuming that the TAF indirectly influences vessel proliferation.

Following Liotta *et al.* [14], let $n_1(\mathbf{x}, t)$ be the tumour cell density and $n_2(\mathbf{x}, t)$ be the surface area of capillary vessels per unit volume. Conservation of mass gives us

$$\frac{\partial n_1}{\partial t} + \nabla \cdot \mathbf{J}_1 = f(n_1, n_2), \quad (1)$$

$$\frac{\partial n_2}{\partial t} + \nabla \cdot \mathbf{J}_2 = g(n_1, n_2), \quad (2)$$

where \mathbf{J}_i , $i = 1, 2$, is the flux and $f(n_1, n_2)$ and $g(n_1, n_2)$ are functions describing interactions between tumour cells and capillary vessels. These also contain source and sink terms which will be made explicit below. We assume that there is a small amount of random motion of both tumour cells and capillary vessels which can be modelled by a diffusion term with constant diffusion coefficient; i.e., $\mathbf{J}_i = -D_i \nabla n_i$, $i = 1, 2$. Many mathematical models of prevascular tumours rely solely on diffusion as a mechanism for tumour growth [15,16]. In a malignant tumour, there is a clear movement of tumour cells into the capillary mass. Indeed, the appearance of metastases is a clear indication that tumour cells have invaded the blood system [1]. We assume that tumour cells react to blood vessels in a similar manner to that of 'taxis'; that is, the tumour cells move up a gradient of capillary vessels. Hence, the flux of tumour cells is given by

$$\mathbf{J}_1 = \mathbf{J}_{\text{diffusion}} + \mathbf{J}_{\text{taxis}} = -D_1 \nabla n_1 + \chi n_1 \nabla n_2, \quad (3)$$

where, for simplicity, we assume χ is a constant.

The functions f and g are carefully chosen to describe the particular behaviour and interaction of the tumour cells and blood vessels.

For the tumour proliferation rate, we assume that during its avascular stage the tumour has reached its maximum size and has become dormant. Folkman [4] reports that tumour cells lying nearest to a capillary have the highest [^3H] thymidine labelling index and that the index decreases as the distance from the capillary increases. Hence, we assume that the proliferation rate is dependent on the surface area of capillary vessels, n_2 . We also assume that, given an adequate supply of nutrients, the proliferation of tumour cells is very rapid since tumour-induced angiogenesis will continue indefinitely until the tumour is eradicated or the host dies [4]. Hence, we model the tumour cell proliferation rate by rn_1n_2 .

The vascular proliferation rate is assumed to be of a Michaelis-Menten form which saturates as n_2 increases, so that there is a finite limit to the proliferation rate. The normal turnover rate of endothelial cells is negligible on the time-scale that we are considering [8]. In normal endothelium, the labelling index was found to be as low as 0.01% per hour in some cases [17]. The proliferation of capillary vessels is initiated by the release of TAF and so is dependent on the density of tumour cells n_1 . We therefore take the vessel proliferation term to be $Sn_1n_2/(\beta + n_2)$.

In this model we assume that the main cause of tumour cell death is nutrient deficiency [17]. Capillary vessels may fail to reach some parts of the tumour or tumour cell overcrowding and high internal pressure may cause vessels to collapse [17,18]. If the oxygen concentration in a tumour cell is inadequate for normal cell functions, the cell becomes hypoxic which leads to a reduction in cell activity. A hypoxic cell can return to normal if nutrient levels increase but will eventually die if deprived of oxygen for too long. In this model we assume that once a cell has become hypoxic it will subsequently die. In Section 4 we will suggest a way of incorporating temporarily hypoxic tumour cells into a model. Let N_2 be some reference vessel surface area such as the surface area per unit volume at the point of vascularization. We choose $\alpha n_1(1 - \tanh((n_2 - N_2)/N_2))$ as our tumour cell death term, as this gives us a smooth switch from high to low death as n_2 increases, which is qualitatively what is desired. Furthermore, there is a finite limit to tumour cell death as $n_2 \rightarrow 0$, which suggests that the tumour returns to its dormant state as nutrients decrease (see Figure 1a).

The death of vasculature is mainly due to overcrowding of vessels and tumour cells, and hence we would expect a sharp increase in vessel death as n_2 increases and also a term which depends on n_1 . We therefore chose $An_1n_2^2/(B + n_2^2)$ as our vessel death term. This term has previously been used to describe spruce budworm death due to overcrowding and predation [19]. In a similar manner, tumour cells invade the blood vessels which collapse due to the massive increase in tumour volume (see Figure 1b).

Hence, the reaction terms f and g are

$$f(n_1, n_2) = rn_1n_2 - \alpha n_1 \left(1 - \tanh \frac{(n_2 - N_2)}{N_2} \right), \quad (4)$$

$$g(n_1, n_2) = \frac{Sn_1n_2}{\beta + n_2} - \frac{An_1n_2^2}{B + n_2^2}. \quad (5)$$

As stated in the introduction, we assume that the tumour is a solid spherical mass and that all growth is in the radial direction only; i.e., we have radial symmetry. If R is the distance from the centre of the tumour, under the assumptions made on f and g , and from equations (1) and (2), we therefore have the following partial differential equation model for vascular tumour growth and invasion:

$$\frac{\partial n_1}{\partial t} = \frac{D_1}{R^2} \frac{\partial}{\partial R} \left(R^2 \frac{\partial n_1}{\partial R} \right) - \frac{1}{R^2} \frac{\partial}{\partial R} \left(R^2 \chi n_1 \frac{\partial n_2}{\partial R} \right) + rn_1n_2 - \alpha n_1 \left(1 - \tanh \frac{(n_2 - N_2)}{N_2} \right), \quad (6)$$

$$\frac{\partial n_2}{\partial t} = \frac{D_2}{R^2} \frac{\partial}{\partial R} \left(R^2 \frac{\partial n_2}{\partial R} \right) + \frac{Sn_1n_2}{\beta + n_2} - \frac{An_1n_2^2}{B + n_2^2}. \quad (7)$$

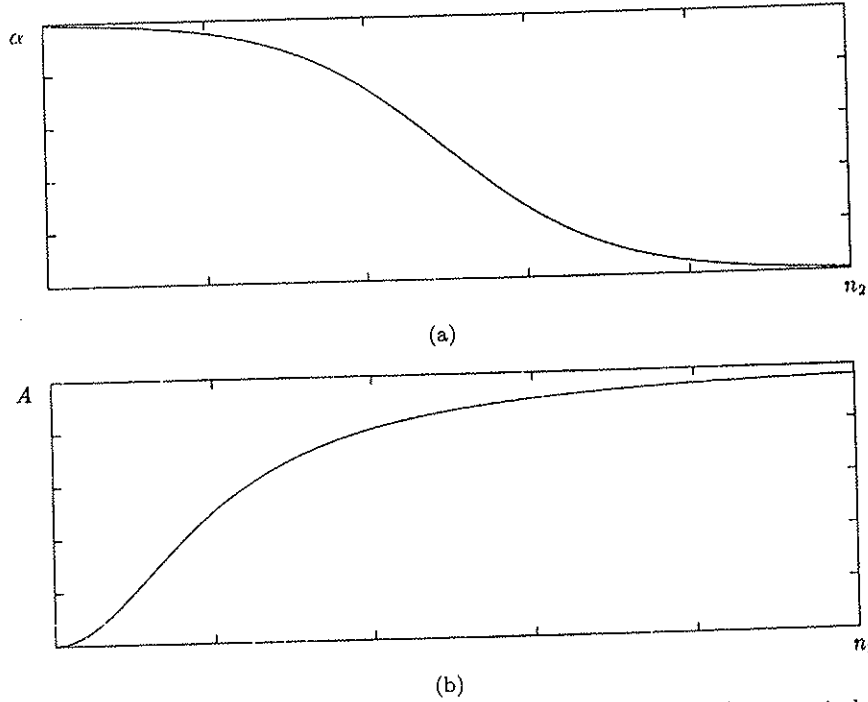


Figure 1. The qualitative forms of the two death terms. Figure (a) is a typical tumour cell death term $\alpha(1 - \tanh((n_2 - N_2)/N_2))$ while Figure (b) shows the vessel death term $An_2^2/B + n_2^2$.

We now nondimensionalize the above system in the usual way. Let L be some reference length, such as the distance from the tumour boundary to the parent vessel, let $\tau = L^2/D_2$ be our reference time, and N_1 a reference tumour cell density. By making the following substitutions,

$$\begin{aligned} n_1^* &= \frac{n_1}{N_1}, & n_2^* &= \frac{n_2}{N_2}, & R^* &= \frac{R}{L}, & t^* &= \frac{t}{\tau}, \\ D &= \frac{D_1}{D_2}, & \chi^* &= \frac{\chi N_2}{D_2}, & r^* &= r N_2 \tau, & \alpha^* &= \alpha \tau, \\ \beta^* &= \frac{\beta}{N_2}, & B^* &= \frac{B}{N_2^2}, & A^* &= \frac{A N_1 \tau}{N_2}, & S^* &= \frac{S N_1 \tau}{N_2}, \end{aligned}$$

and dropping the asterisks for notational convenience, we obtain the dimensionless system

$$\frac{\partial n_1}{\partial t} = \frac{D}{R^2} \frac{\partial}{\partial R} \left(R^2 \frac{\partial n_1}{\partial R} \right) - \frac{1}{R^2} \frac{\partial}{\partial R} \left(R^2 \chi n_1 \frac{\partial n_2}{\partial R} \right) + r n_1 n_2 - \alpha n_1 (1 - \tanh(n_2 - 1)), \quad (8)$$

$$\frac{\partial n_2}{\partial t} = \frac{1}{R^2} \frac{\partial}{\partial R} \left(R^2 \frac{\partial n_2}{\partial R} \right) + \frac{S n_1 n_2}{\beta + n_2} - \frac{A n_1 n_2^2}{B + n_2^2}. \quad (9)$$

To close the system, we impose the following boundary conditions:

$$\begin{aligned} \text{at } R = 0, & \quad \frac{\partial n_1}{\partial R} = 0, & \quad \frac{\partial n_2}{\partial R} = 0, \\ \text{at } R = 1, & \quad \frac{\partial n_1}{\partial R} = 0, & \quad n_2 = 1. \end{aligned}$$

The first set of boundary conditions arises naturally from the symmetry of the system. The position $R = 1$ corresponds to the location of the parent vessels (e.g., *limbus*). Once the tumour cells reach the right-hand boundary the assumptions of the model will no longer hold, since other interactions become important (e.g., the invasion of the limbus by the tumour cells). Various initial conditions will be considered in Section 2.2.

2.1. Estimation of Parameters

Whenever possible experimental data was used to estimate our parameter values. Where this was difficult, we chose parameters that gave the correct qualitative behaviour of the tumour cells and the blood vessels.

A summary of data on corneal implants was given by Balding and McElwain [20]. A tumour will successfully induce angiogenesis if placed at a distance of 0.8 mm [6] to 3 mm [5] from the limbal vessels. The time for vascularization is approximately 8 to 12 days [5,6,10]. This gives a value for $D_2 \simeq 10^{-7} \text{ cm}^2 \text{ s}^{-1}$, for $\tau \simeq 10$ days and $L \simeq 0.3$ cm. Sherratt and Murray [21] estimated the diffusion coefficient of cells in their model of epidermal wound healing. They used diffusion coefficients ranging from $3 \times 10^{-9} \text{ cm}^2 \text{ s}^{-1}$ – $6.9 \times 10^{-11} \text{ cm}^2 \text{ s}^{-1}$. In their study of individual endothelial cells, Stokes and Lauffenburger [22] measured the motility parameters for endothelial cells. The mean random motility coefficient for endothelial cells migrating in α FGF, was $7.1 \pm 2.7 \times 10^{-9} \text{ cm}^2 \text{ s}^{-1}$. A reasonable estimate of the diffusion coefficient of tumour cells would be in the range 10^{-9} to $10^{-11} \text{ cm}^2 \text{ s}^{-1}$. This would give a range for D of 10^{-4} to 10^{-2} . We would expect the diffusion of tumour cells to be small in comparison with the directed movement of the tumour cells in response to a gradient of blood vessels, which is clear from experimental studies. We therefore, chose the taxis coefficient to be ten times that of the tumour cell diffusion, so that, with $N_2 = 10^3$, an approximate range for χ is 1 to 100. The parameter r corresponds to the tumour proliferation rate, which we would expect to be fairly high. If tumour cell proliferation was about 0.1% per hour, then $r \sim O(10^2)$. The maximum death rate in the absence of capillary vessels is represented by α . Denekamp [17] stated that the lifespan of a nutrient-deprived hypoxic cell is 5 to 10 hours. The proportion of hypoxic cells in a tumour can be up to 80%. Hence, a reasonable range for α is 1–20. For the capillary vessels, the parameters S and A represent the maximum proliferation and death rates respectively, whereas, β and B are measures of the critical value at which proliferation or death is switched on. A low value of β or B means a low threshold. The tumour's vasculature is highly vulnerable [8,17], and hence, we chose a low death threshold value, $B = 0.01$, and a high maximum death rate, $A = 100$, in comparison to the proliferation threshold, $\beta = 1$, and the maximum proliferation rate $S = 10$.

2.2. Numerical Simulations

The system of equations was solved using a routine available from the NAG library which integrates the system using the method of lines and Gear's method. Three different sets of initial conditions were used (Figure 2).

In the first case, we tried similar initial conditions to those used by Liotta *et al.* [14] in their model of tumour vascular growth, i.e., unit step functions (Figure 2a). Assuming that the tumour is placed at a distance of 3 mm from the parent vessel and that its radius is about 1 mm, we take the tumour boundary to be situated at $R = 0.25$. The results are given in Figure 3. Figure 3a shows a peak of tumour cells moving across the domain towards the parent vessel, and there is a decline in tumour cell density at the centre, indicating that a necrotic core has developed. Figure 3b shows that the capillary vessels have infiltrated the tumour mass and have slightly regressed from the advancing front of tumour cells. However, the vessels have not, as would be expected, degenerated at the centre of the tumour.

In the second case, a more realistic initial profile for the tumour cells was chosen with a Gaussian distribution of cells centred at $R = 0.2$ (Figure 2b). This corresponds to a newly vascularized tumour nodule with central necrosis surrounded by a layer of live proliferating cells, since only proliferating cells invade. Again, the results show (Figure 4a) a peak of advancing tumour cells penetrated by capillaries. Figure 4b shows that the regression of vessels is slightly more pronounced, and after time $t = 0.03$, the density of vessels at the centre of the tumour begins to decrease, which is an improvement on the simulations of Figure 3b.

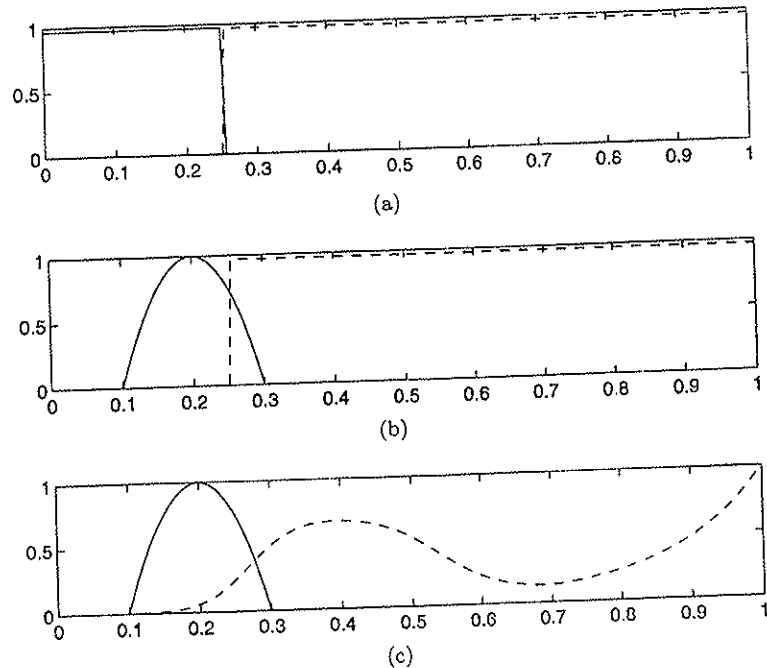


Figure 2. The three different initial conditions used to test the model. The solid line represents the tumour cell distribution and the dashed line represents the vessel density. In Figure (a) we have a block distribution of tumour cells and vessels. In Figure (b) we have a Gaussian distribution of tumour cells centred at 0.2. In Figure (c) we have the same Gaussian distribution for the tumour cells but for the vessels we have taken a profile from the model of angiogenesis by Chaplain and Stuart [23].

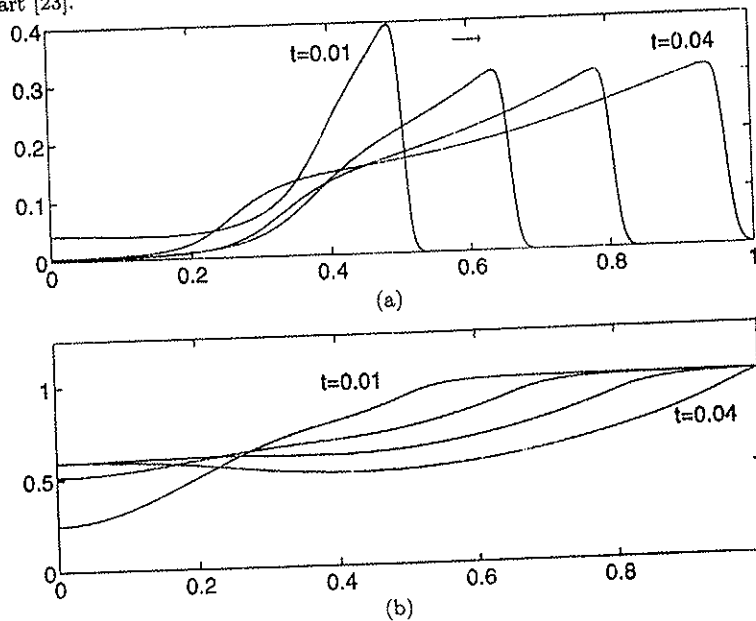


Figure 3. With block initial conditions for the tumour cells and the vessels the system evolves as shown above. Figure (a) shows the tumour cells distribution and Figure (b) the vessels. Plots were taken at times $t = 0.01, 0.02, 0.03$ and 0.04 . Parameters values were $D = 0.01, \chi = 10, r = 100, \alpha = 10, S = 10, \beta = 1, A = 100, B = 0.01$.

Finally, we took an initial profile of capillary vessels from a model of angiogenesis by Chaplain and Stuart [23] (Figure 2c). The taxis coefficient χ is reduced in order to allow more time for the overcrowding to take effect and also the tumour cell proliferation rate r was increased. Figure 5a

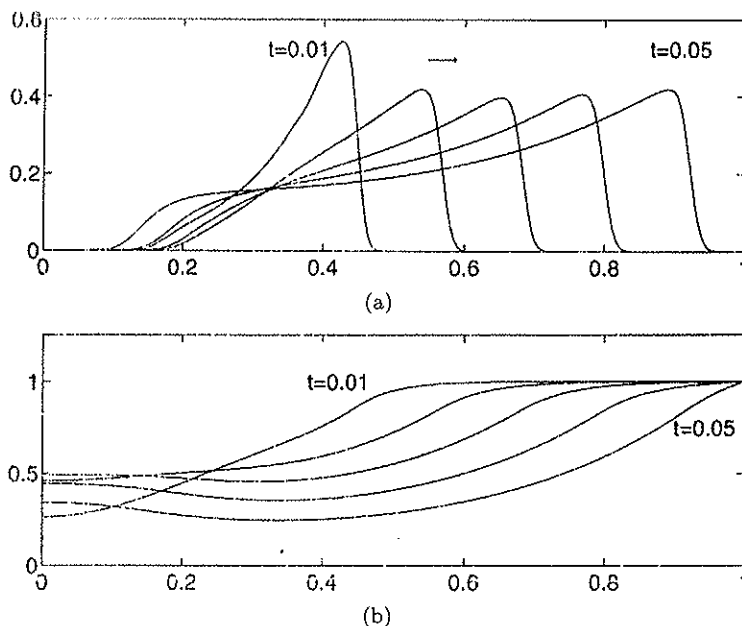


Figure 4. With a Gaussian distribution of tumour cells and block initial conditions for the vessels the system evolves as shown. Figure (a) shows the tumour cell density while Figure (b) shows the vessel distribution. Plots were taken at times $t = 0.01, 0.02, 0.03, 0.04$ and 0.05 . Parameters values were $D = 0.01, \chi = 5, \tau = 100, \alpha = 10, S = 10, \beta = 1, A = 100, B = 0.01$.

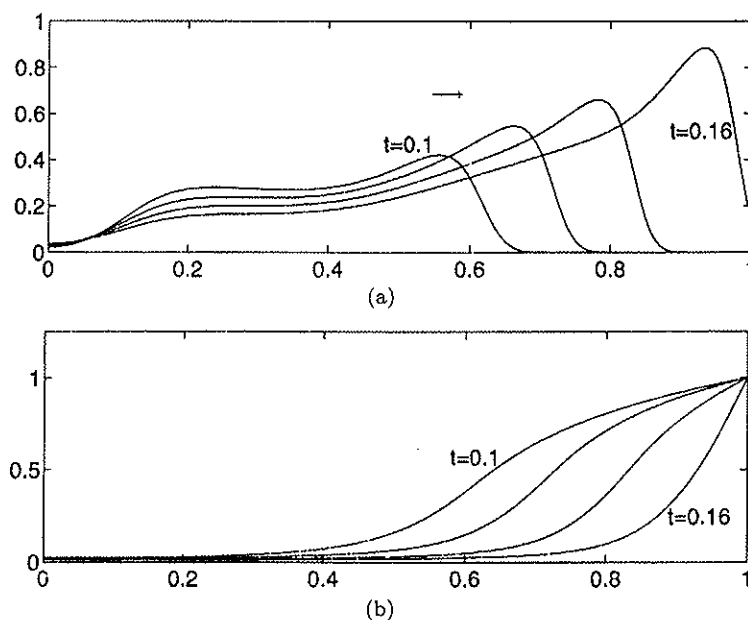


Figure 5. With an initial profile for the vessels taken from Chaplain and Stuart [23] the system will evolve as shown. Figure (a) shows the tumour cell density while Figure (b) shows the vessel distribution. Plots were taken at times $t = 0.1, 0.12, 0.14$ and 0.16 . Parameters values were $D = 0.01, \chi = 1, \tau = 200, \alpha = 7, S = 10, \beta = 1, A = 100, B = 0.01$.

shows an advancing peak of tumour cells and a substantial increase in tumour cell density with time. Figure 5b shows that the capillaries have penetrated the tumour mass but have collapsed at the centre and the vasculature within the tumour has regressed considerably.

We note that the qualitative form of the numerical solutions are wave-like. We can estimate the speed of the wave by examining the numerical solutions. For the first two simulations (Figures 3 and 4), we estimate that the dimensionless wave speed varies between 11–15. With $L = 0.3$ cm as

ain
the
5a

a reference length and $\tau = 10$ days as a reference time, this gives a speed of invasion in the range of 3.3–4.5 mm/day, which is quite high. In the last simulation (Figure 5), which has the most realistic initial conditions and which best captures the key behaviour of the growing tumour, the dimensionless wave speed is approximately 4.5–5. This corresponds to an invasion speed of 1.4 mm/day–1.5 mm/day. This is not unreasonable, given the simplicity of the model, though slightly overestimated, in comparison to experimental observations of 0.2–0.5 mm/day [5] and 0.4–0.7 mm/day [24]. We will suggest ways of reducing the wave speed in the discussion. In the next section, we will investigate the possibility of travelling wave solutions with constant speed and profile.

3. TRAVELLING WAVE ANALYSIS

In this section, we conduct a travelling wave analysis of the system of partial differential equations (8) and (9). We modify the original model by replacing the proliferation term for the blood vessels by the logistic growth term $Sn_2(1 - n_2)$, where, once again the parameter S is dimensionless. The use of this term can be justified by assuming that the blood vessels have been saturated by TAF, and hence, the proliferation of vessels is independent of tumour cell density. Given that the rate of growth of the vascularized tumour is rapid, the tumour mass rapidly increases in size [5,6]. We therefore conduct the travelling wave analysis using Cartesian coordinates as follows:

$$\frac{\partial n_1}{\partial t} = D \frac{\partial^2 n_1}{\partial R^2} - \chi \frac{\partial}{\partial R} \left(n_1 \frac{\partial n_2}{\partial R} \right) + rn_1 n_2 - \alpha n_1 (1 - \tanh(n_2 - 1)), \quad (10)$$

$$\frac{\partial n_2}{\partial t} = \frac{\partial^2 n_2}{\partial R^2} + Sn_2(1 - n_2) - \frac{An_1 n_2^2}{B + n_2^2}. \quad (11)$$

The spatially homogeneous steady states are given by $(0, 0)$, $(0, 1)$ and (n_1^*, n_2^*) where

$$n_1^* = \frac{S(1 - n_2^*)(B + n_2^{*2})}{An_2^*}, \quad (12)$$

and n_2^* uniquely satisfies

$$rn_2^* - \alpha(1 - \tanh(n_2^* - 1)) = 0. \quad (13)$$

We look for solutions of the form $N_1(z) = n_1(R, t)$, $N_2(z) = n_2(R, t)$, where $z = R - ct$, c being a constant positive wave speed, so that the waves travel to the right. Using the notation ' to denote differentiation with respect to z , we obtain a fourth order system of ordinary differential equations

$$-cN_1' = DN_1'' - \chi(N_1 N_2')' + rN_1 N_2 - \alpha N_1(1 - \tanh(N_2 - 1)), \quad (14)$$

$$-cN_2' = N_2'' + SN_2(1 - N_2) - \frac{AN_1 N_2^2}{B + N_2^2}. \quad (15)$$

The appropriate boundary conditions are given below, i.e., nonnegative solutions satisfying

$$\begin{aligned} N_1(-\infty) &= n_1^*, & N_1(+\infty) &= 0, \\ N_2(-\infty) &= n_2^*, & N_2(+\infty) &= 1, \\ N_1'(\pm\infty) &= 0, & N_2'(\pm\infty) &= 0. \end{aligned} \quad (16)$$

Waves satisfying (16) can be described as 'waves of invasion.' In this case, we have one population at its carrying capacity. Introducing a small amount of another species, the system evolves to a new steady state of coexistence where the original population has decreased and the new species has increased. From this description of invasion, we infer $n_2^* < 1$. In the biological situation that we are considering, tumour cells invade a population of endothelial cells.

We analyse the system (14) and (15) by considering two cases. First, we will simplify the system by setting $D = 0$, which is the limiting case of D small. In this case, the vessels are diffusing much faster than the tumour cells. This implies that there is little random motion of tumour cells, therefore, the emphasis is on the directed movement of tumour cells into the capillary vessels. Second, we consider D nonzero.

CASE 1. $D = 0$. Letting $W = N_2'$, we obtain the following system of three first-order ordinary differential equations:

$$N_1' = \left(\frac{1}{\chi W - c} \right) \left[rN_1N_2 - \alpha N_1 (1 - \tanh(N_2 - 1)) + \chi N_1 \left(SN_2(1 - N_2) - \frac{AN_1N_2^2}{B + N_2^2} + cW \right) \right], \quad (17)$$

$$N_2' = W, \quad (18)$$

$$W' = \frac{AN_1N_2^2}{B + N_2^2} - SN_2(1 - N_2) - cW. \quad (19)$$

To remove the singularity at $W = c/\chi$, let $(\chi W - c) \frac{d}{dz} = \frac{d}{d\xi}$. Hence, we obtain the following system:

$$\frac{dN_1}{d\xi} = rN_1N_2 - \alpha N_1 (1 - \tanh(N_2 - 1)) + \chi N_1 \left(SN_2(1 - N_2) - \frac{AN_1N_2^2}{B + N_2^2} + cW \right), \quad (20)$$

$$\frac{dN_2}{d\xi} = W(\chi W - c) \quad (21)$$

$$\frac{dW}{d\xi} = \left(\frac{AN_1N_2^2}{B + N_2^2} - SN_2(1 - N_2) - cW \right) (\chi W - c). \quad (22)$$

We carry out a phase plane analysis in the usual way by linearizing about each critical point to obtain a system of the form

$$\frac{d\mathbf{X}}{d\xi} = A\mathbf{X}, \quad \text{where } \mathbf{X} = (N_1, N_2, W)^T$$

and A is a 3×3 Jacobian matrix which has been evaluated at the critical point. The eigenvalues are then given by $\det(A - \lambda I) = 0$. Using the notation A_{ij} to denote the element in the i^{th} row and j^{th} column of the matrix A , we obtain

$$\lambda^3 - \lambda^2(A_{11} + A_{33}) + \lambda(A_{11}A_{33} - A_{13}A_{31} - A_{23}A_{32}) + A_{11}A_{23}A_{32} - A_{12}A_{23}A_{31} = 0, \quad (23)$$

since A_{21} and A_{22} are always zero when evaluated at any of the critical points. The analysis of this phase space is given in the Appendix. A summary of the results is as follows.

- The critical point $(0,0,0)$ is a stable node if $c^2 < \alpha(1 + \tanh 1) < S$. Otherwise, the critical point is a saddle point.
- For nonnegative solutions passing through $(0,0,0)$, the parameters must satisfy equations (32) and (33) as given in the Appendix.
- Since $r > \alpha$ from equation (13), the critical point $(0,1,0)$ is a saddle.
- For nonnegative solutions passing through $(0,1,0)$, the parameters must satisfy equations (35) and (36).
- The critical point $(n_1^*, n_2^*, 0)$ is a stable node if $c^2 < \chi S n_2^*(1 - n_2^*)$; otherwise it is a saddle.

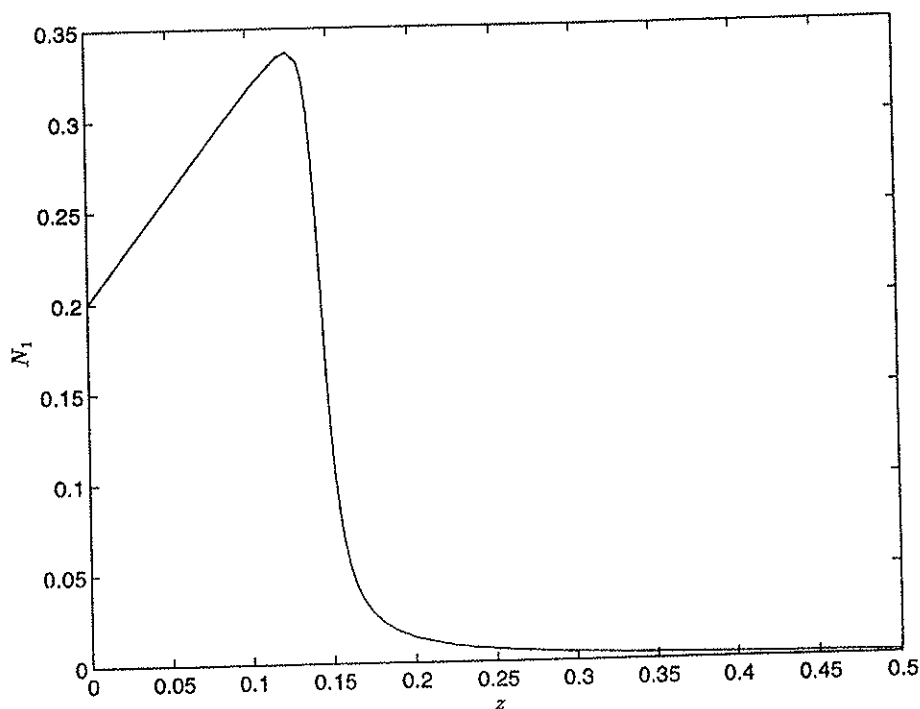


Figure 6. Profile of tumour cells invading tissue obtained from numerical solution to (20)–(22).

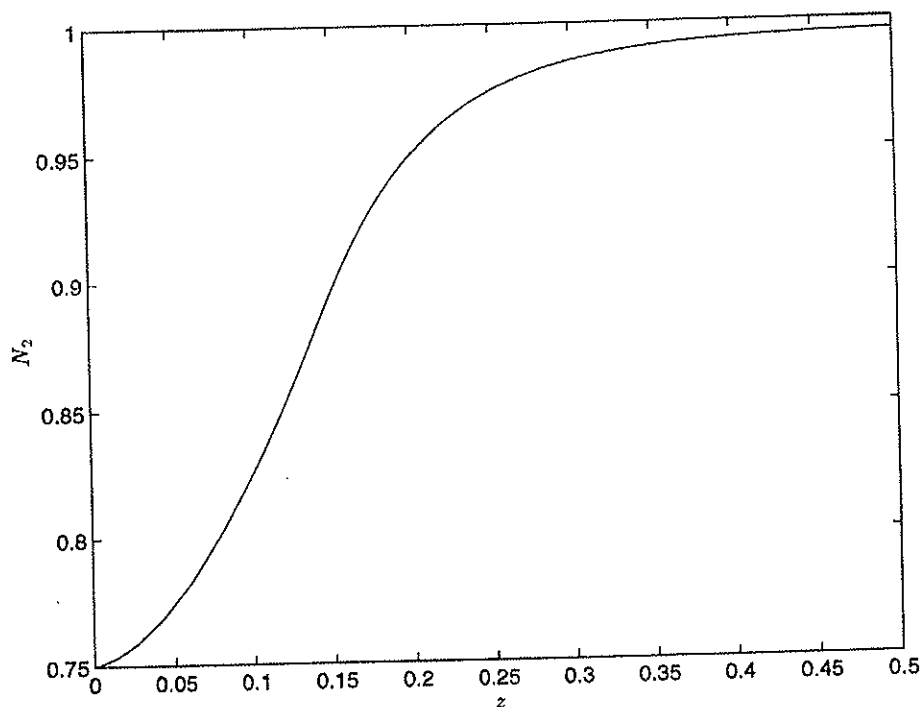


Figure 7. Profile of vessel density being invaded obtained from numerical solution to (20)–(22).

We solved the system of equations (20)–(22) using an ODE solver implemented in MATLAB with the parameters $D = 0$, $\chi = 10$, $r = 100$, $\alpha = 10$, $S = 10$, $\beta = 1$, $A = 100$, $B = 0.01$ and the wavespeed $c = 16.9$ which was derived from conditions (35) and (36). Figures 6 and 7 show the profiles of the wave front for the tumour cell density and the vessel density, respectively.

Qualitatively, they illustrate the advance of the region of proliferating tumour cells with the collapse of the vasculature in its wake.

CASE 2. $D > 0$. Letting $U = N_1'$ and $V = N_2'$, we obtain the following system of four ODE's:

$$N_1' = U, \quad (24)$$

$$N_2' = V, \quad (25)$$

$$U' = \frac{1}{D} \left[\chi \left(UV + N_1 \left(\frac{AN_1N_2^2}{B + N_2^2} - SN_2(1 - N_2) - cV \right) \right) + \alpha N_1(1 - \tanh(N_2 - 1)) - rN_1N_2 - cU \right], \quad (26)$$

$$V' = \frac{AN_1N_2^2}{B + N_2^2} - SN_2(1 - N_2) - cV. \quad (27)$$

We carry out a phase plane analysis in the usual way by linearizing about each critical point to obtain a system of the form

$$\frac{d\mathbf{X}}{dz} = A\mathbf{X}, \quad \text{where } \mathbf{X} = (N_1, N_2, U, V)^T$$

and A is a 4×4 Jacobian matrix which has been evaluated at the critical point. The eigenvalues are then given by $\det(A - \lambda I) = 0$. Using the notation A_{ij} to denote the element in the i^{th} row and j^{th} column of the matrix A , we obtain

$$\lambda^4 + \lambda^3(c - A_{33}) - \lambda^2(A_{42} + A_{31} + cA_{33}) + \lambda(A_{33}A_{42} - cA_{31} - A_{34}A_{41}) + A_{31}A_{42} - A_{32}A_{41} = 0. \quad (28)$$

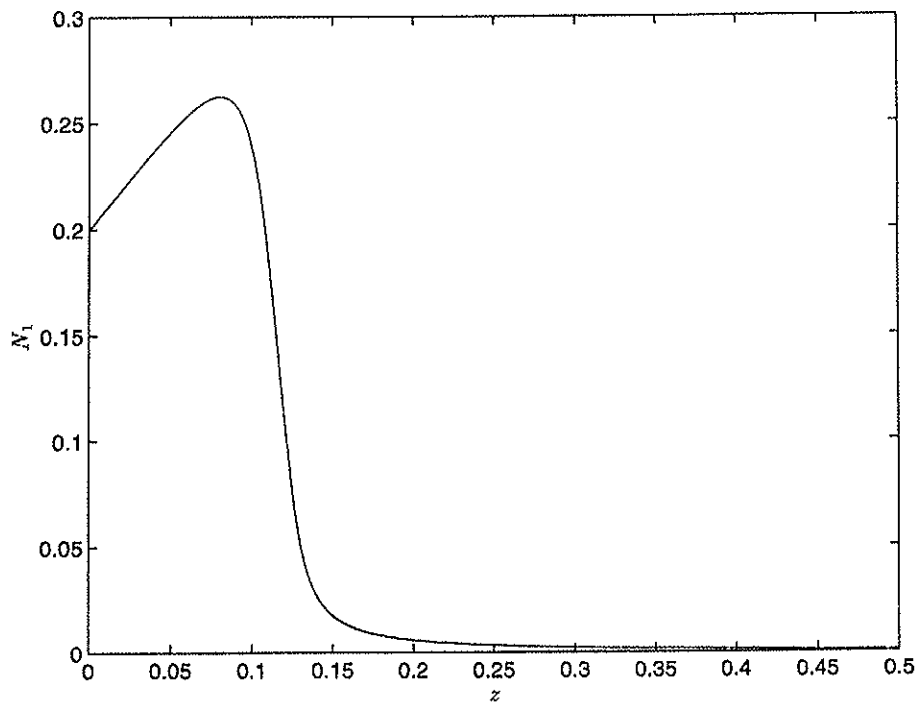


Figure 8. Profile of tumour cells invading tissue obtained from numerical solution to (24)-(27).

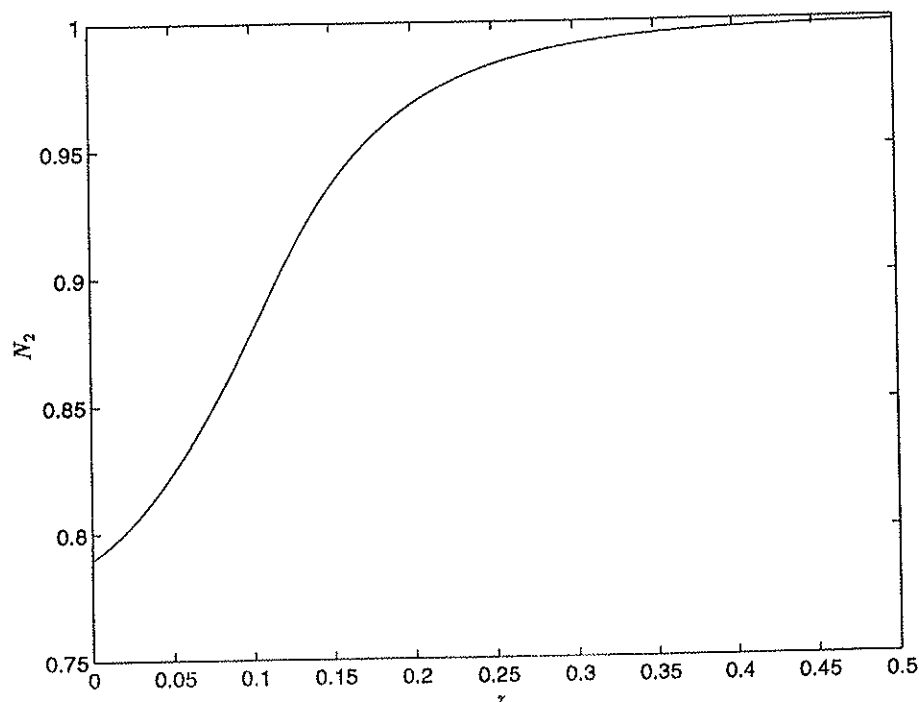


Figure 9. Profile of vessel density being invaded obtained from numerical solution to (24)–(27).

The analysis of this phase space is given in the Appendix. A summary of the results is as follows.

- The condition $S < \alpha(1 + \tanh 1)$ is sufficient to ensure that the critical point $(0,0,0,0)$ has an unstable manifold.
- The critical point $(0,1,0,0)$ is a saddle since $r > \alpha$.
- The critical point $(n_1^*, n_2^*, 0, 0)$ is a stable node if $1/27 > B > 0$ and $c^2 < \chi S n_2^*(1 - n_2^*)$, otherwise it is a saddle.

Again, we solved the system of equations (24)–(27) using MATLAB with the parameters $D = 0.01$, $\chi = 10$, $r = 100$, $\alpha = 10$, $S = 10$, $\beta = 1$, $A = 100$, $B = 0.01$ and the wave speed $c = 15$, which was measured from the original numerical solutions of the PDE's. Figures 8 and 9 show the profiles of the wave front for the tumour cell density and the vessel density, respectively. Once again the figures illustrate the advancing front of invading tumour cells leaving behind a compressed vasculature in its wake.

4. DISCUSSION

We have developed a simple minimal mathematical model which has captured the key initial events of vascular tumour growth such as the migrating front of tumour cells, necrosis and the regression of blood vessels. The advance of tumour cells across the host-tissue field is attributed to a combination of diffusion, active migration and proliferation of tumour cells. Liotta *et al.* [14] explains central necrosis as a failure of new blood vessels to reach the centre of the tumour fast enough. However, shortly after vascularization, the whole of the tumour is criss-crossed by capillaries [8], with necrosis reappearing later. Hence, in this model the development of a necrotic core is due to overcrowding and the eventual collapse of the blood vessels.

We note that the model is necessarily a simple one and neglects many other features of tumour growth. For example, we do not consider the effect of extravascular pressure or the compression of host tissue which can obstruct the flow of blood to the tumour cells [4]. Denekamp [17] reports on the possibility of cyclic hypoxia, that is the temporary opening and closing of vessels for a few seconds or even for a few hours. We could include temporarily and permanently hypoxic cells

by developing an age-structured model. This would involve two age classes for the tumour cells with 'young' proliferating cells in one class and 'old' reduced activity cells in the other, with cells switching from class to class whenever nutrient levels were above or below some threshold value.

Alternatively, we could develop a mechanical model which focuses on cell-matrix interactions [19]. In the numerical simulations, the wave speed was slightly larger than that observed experimentally [5,24]. No doubt this is due to the fact that the model is simple and does not consider other factors which may moderate the movement of the tumour cells. The extracellular matrix has an important role to play in tumour growth, especially invasive growth, since it can influence cell adhesion and motility [1,11,25,26].

The model also assumes radial symmetry. It is unusual for tumours to grow outward to an equal extent in all directions except when grown in a homogeneous environment, e.g., in the liver. Studies on multicellular spheroids [27] have shown that there is heterogeneity in both the cells and the environment. A more realistic model ought to take this fact into account.

Nevertheless, in spite of these simplifications, the model produces results which are in good qualitative agreement with *in vivo* observations, and gives a quantitative estimate of the invasive speed which is reasonable given the simplicity of the model. By improving the model as suggested above, no doubt, better results and predictions will be obtained.

APPENDIX A ANALYSIS OF THE THREE-DIMENSIONAL PHASE SPACE

A.1. At the Critical Point (0, 0, 0)

$$\begin{aligned} A_{11} &= -\alpha(1 + \tanh 1), & A_{12} &= 0, & A_{13} &= 0, & A_{23} &= -c, \\ A_{31} &= 0, & A_{32} &= Sc, & A_{33} &= c^2. \end{aligned}$$

Hence, the eigenvalues are given by the roots of

$$p(\lambda) = \lambda^3 + \lambda^2 a_1 + \lambda a_2 + a_3, \tag{29}$$

where

$$\begin{aligned} a_1 &= \alpha(1 + \tanh 1) - c^2, \\ a_2 &= c^2(S - \alpha(1 + \tanh 1)), \\ a_3 &= Sc^2\alpha(1 + \tanh 1). \end{aligned}$$

If $c^2 < \alpha(1 + \tanh 1) < S$ then the origin is a stable node. Otherwise, the critical point is a saddle point.

For nonnegative solutions, we require these roots to be real. We must impose the conditions $\alpha_1 > 0$ and $\beta_1 = 0$ [19], where

$$\alpha_1 = \left(\frac{a_1}{3}\right)^2 - \left(\frac{a_2}{3}\right), \tag{30}$$

$$\beta_1 = 2\left(\frac{a_1}{3}\right)^3 - \frac{a_1 a_2}{3} + a_3. \tag{31}$$

From the first condition we have

$$\alpha^2(1 + \tanh 1)^2 + c^4 - 3c^2S + c^2\alpha(1 + \tanh 1) > 0. \tag{32}$$

A sufficient condition to satisfy $\alpha_1 > 0$ is $c^2 > 3S$ or $\alpha(1 + \tanh 1) > 3S$.

From the second condition $\beta_1 = 0$, we have

$$2(\alpha(1 + \tanh 1))^3 + 3(\alpha(1 + \tanh 1))^2(3 - 2c^2) + 3\alpha(1 + \tanh 1)(2c^4 + 3(3S - 1)c^2 - 3S) + c^2(9S - 2c^4) = 0. \quad (33)$$

Since α is real and positive, as a minimum requirement, we need the above polynomial to have one positive root. By Descartes Rule of Signs we require

$$3 > 2c^2, \quad 2c^4 + 3(3S - 1)c^2 - 3S > 0, \quad 2c^4 > 9S.$$

From the second condition for c^2 real and positive we must have $3S < 1$. Hence, combining these conditions $3/2 > c^2 > \sqrt{3/2}$ is sufficient for α real and positive.

A.2. At the Critical Point (0, 1, 0)

$$A_{11} = r - \alpha, \quad A_{12} = 0, \quad A_{13} = 0, \quad A_{23} = -c, \\ A_{31} = \frac{-A}{B+1}, \quad A_{32} = -Sc, \quad A_{33} = c^2.$$

Hence, the eigenvalues are given by

$$\lambda^3 + \lambda^2(\alpha - r - c^2) + \lambda c^2(r - \alpha - S) + Sc^2(r - \alpha) = 0, \quad (34)$$

i.e., the roots of $p(\lambda) = \lambda^3 + \lambda^2 a_1 + \lambda a_2 + a_3$, where

$$a_1 = \alpha - r - c^2, \quad a_2 = c^2(r - \alpha - S), \quad a_3 = Sc^2(r - \alpha).$$

(0, 1, 0) is a saddle point. If $r > \alpha$, the polynomial $p(\lambda)$ will have two positive roots and one negative root. If $\alpha > r$ we will have one positive root and two negative roots. However, by examination of equation (13) combined with the condition for invasion $n_2^* < 1$, we conclude that $r > \alpha$.

Again we must impose conditions on our parameters so that the solutions are nonnegative; i.e., the eigenvalues must be real. From the condition $\alpha_1 > 0$ where α_1 is given by (30) we obtain

$$\alpha^2 + r^2 + c^4 + 3Sc^2 - 2r\alpha > 0. \quad (35)$$

$r > 2\alpha$ is a sufficient but not necessary condition which satisfies (35). From $\beta_1 = 0$ where β_1 is given by (31), we obtain

$$\frac{2}{27} [-(r - \alpha) - c^2]^3 - \frac{c^2}{3} [-(r - \alpha) - c^2] [(r - \alpha) - S] + Sc^2(r - \alpha) = 0, \\ \frac{2}{27} [-(r - \alpha) - c^2]^3 - \frac{c^2}{3} [-(r - \alpha) - c^2] [(r - \alpha) - S] + Sc^2(r - \alpha) = 0.$$

After some algebra this becomes

$$2(r - \alpha)^3 - 3c^2(r - \alpha)^2 - c^2(r - \alpha)(18S + 6c^2) + c^4(2c^2 + 9S) = 0. \quad (36)$$

A.3. At the Third Critical Point ($n_1^*, n_2^*, 0$)

Using equations (12) and (13), the eigenvalues are given by the cubic

$$\lambda^3 + \lambda^2 \left[\chi n_2^* S (1 - n_2^*) - c^2 \right] + \lambda Sc^2 \left[\frac{2n_2^* (1 - n_2^*)}{(B + n_2^{*2})^2} [n_2^* - \chi (B + n_2^{*2})] - 1 \right] \\ + c^2 n_2^* S (1 - n_2^*) [r + \alpha \operatorname{sech}^2(n_2^* - 1)] = 0, \quad (37)$$

i.e., the roots of $p(\lambda) = \lambda^3 + \lambda^2 a_1 + \lambda a_2 + a_3$ where

$$\begin{aligned} a_1 &= \chi n_2^* S (1 - n_2^*) - c^2, \\ a_2 &= S c^2 \left[\frac{2n_2^* (1 - n_2^*)}{(B + n_2^{*2})^2} [n_2^* - \chi (B + n_2^{*2})] - 1 \right], \\ a_3 &= c^2 n_2^* S (1 - n_2^*) [r + \alpha \operatorname{sech}^2 (n_2^* - 1)]. \end{aligned}$$

There are four possible cases, all roots negative, one root positive and two negative, one negative and two positive and all roots positive.

Suppose all the roots are negative. By the Routh-Hurwitz conditions

$$a_1, a_2, a_3 > 0.$$

The condition $n_2^* < 1$ is satisfied and we obtain a bound on the wavespeed; i.e.,

$$c^2 < \chi n_2^* S (1 - n_2^*).$$

Consider the limiting case $a_3 = 0$. Then the roots of $p(\lambda)$ are

$$\lambda = 0, \quad \lambda_{1,2} = -a_1 \pm \sqrt{a_1^2 - 4a_2},$$

The maximum λ_M and minimum λ_m are given by

$$\frac{dp}{d\lambda} = 3\lambda^2 + 2\lambda a_1 + a_2 = 0, \quad \Rightarrow \lambda_{m,M} = \frac{1}{3} \left(-a_1 \pm \sqrt{a_1^2 - 3a_2} \right).$$

These are independent of a_3 . As a_3 increases from zero, $p(\lambda)$ has three real negative roots. There is a critical value of a_3 , a_3^* say, for which two of the roots are equal where

$$a_3^* = \frac{1}{27} \left(a_1 + 2\sqrt{a_1^2 - 3a_2} \right) \left(a_1 - \sqrt{a_1^2 - 3a_2} \right)^2, \tag{38}$$

so for $a_3 > a_3^*$, we have only one real root and two complex roots. Hence, the solutions approach the critical point in an oscillatory manner for $a_3 > a_3^*$ and for $0 < a_3 < a_3^*$ they are monotonic (Figure 10).

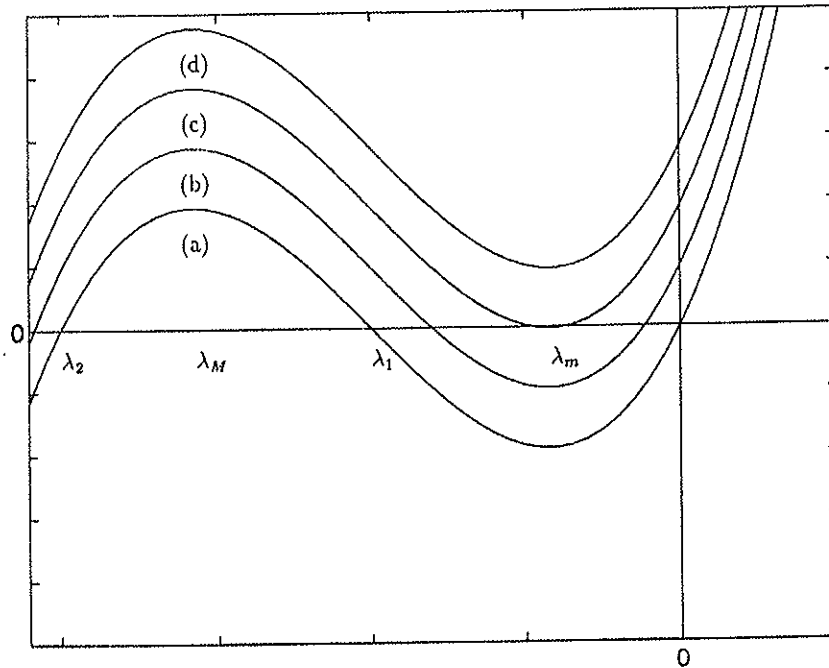


Figure 10. The general form of $p(\lambda)$ as a_3 increases from zero. (a) $a_3 = 0$; (b) $0 < a_3 < a_3^*$; (c) $a_3 = a_3^*$; and (d) $a_3 > a_3^*$.

Suppose that one of the roots of $p(\lambda)$ is positive and two roots are negative. This implies that $a_3 < 0$ and so $n_2^* > 1$, which contradicts our previous assumption. We dismiss this case on the grounds that this situation does not arise in the biological context that we are considering.

Now suppose that two of the roots are positive and one root is negative. Then $a_3 > 0$. Either or both of a_1 and a_2 must be negative. If $a_1 < 0$, then $c^2 > \chi n_2^* S(1 - n_2^*)$. If $a_2 < 0$, then we obtain the inequality

$$(2\chi - 1)n_2^{*4} - 2(\chi + 1)n_2^{*3} + 2(1 + B(\chi - 1))n_2^{*2} - 2\chi Bn_2^* - B^2 < 0.$$

As before, in the case where all the roots were negative, there is a critical value of a_3 . As a_3 increases to this critical value, the two positive real roots become equal. So for $a_3 > a_3^*$ we have a trajectory which oscillates away from (n_1^*, n_2^*) .

Finally, if all the roots are positive we have $a_3 < 0$. Again, we dismiss this case as it is not of biological relevance.

APPENDIX B ANALYSIS OF THE FOUR-DIMENSIONAL PHASE SPACE

B.1. At the Critical Point $(0, 0, 0, 0)$

$$A_{31} = \frac{\alpha}{D}(1 + \tanh 1), \quad A_{32} = 0, \quad A_{33} = -\frac{c}{D},$$

$$A_{41} = 0, \quad A_{42} = -S.$$

Hence, the eigenvalues are given by the roots of

$$p(\lambda) = \lambda^4 + \lambda^3 a_1 + \lambda^2 a_2 + \lambda a_3 + a_4,$$

where

$$a_1 = c + \frac{c}{D},$$

$$a_2 = \frac{c^2}{D} + S + \frac{\alpha}{D}(1 + \tanh 1),$$

$$a_3 = \frac{cS}{D} - \frac{\alpha c}{D}(1 + \tanh 1),$$

$$a_4 = -\frac{\alpha S}{D}(1 + \tanh 1).$$

By examination of a_3 we see that the origin is a saddle. In particular it has an unstable manifold if $S < \alpha(1 + \tanh 1)$, which agrees with the result found in Appendix A.

B.2. At the Critical Point $(0, 1, 0, 0)$

$$A_{31} = \frac{\alpha - r}{D}, \quad A_{32} = 0, \quad A_{33} = -\frac{c}{D},$$

$$A_{34} = 0, \quad A_{41} = \frac{A}{B + 1}, \quad A_{42} = S.$$

Hence, the eigenvalues are given by the roots of

$$p(\lambda) = \lambda^4 + \lambda^3 a_1 + \lambda^2 a_2 + \lambda a_3 + a_4,$$

where

$$a_1 = c + \frac{c}{D},$$

$$a_2 = \frac{1}{D}(c^2 + r - \alpha - DS),$$

$$a_3 = \frac{c}{D}(r - \alpha - S),$$

$$a_4 = \frac{S}{D}(\alpha - r).$$

Since $r > \alpha$, we can see that $(0, 1, 0, 0)$ is always a saddle.

B.3. At the Critical Point $(n_1^*, n_2^*, 0, 0)$

$$\begin{aligned} A_{31} &= \frac{\chi}{D} \left(\frac{2An_1^*n_2^*}{B+n_2^{*2}} - Sn_2^*(1-n_2^*) \right), \\ A_{32} &= \frac{1}{D} (\chi A_{42} - rn_1^* + \alpha n_1^* \operatorname{sech}^2(n_2^* - 1)), \\ A_{33} &= -\frac{c}{D}, \\ A_{34} &= -\frac{\chi cn_1^*}{D}, \\ A_{41} &= \frac{An_2^*}{B+n_2^*}, \\ A_{42} &= \frac{2An_1^*n_2^*}{B+n_2^{*2}} \left(1 - \frac{n_2^{*2}}{B+n_2^{*2}} \right) - S(1-2n_2^*). \end{aligned}$$

Using equations (12) and (13), the eigenvalues are given by the roots of

$$p(\lambda) = \lambda^4 + \lambda^3 a_1 + \lambda^2 a_2 + \lambda a_3 + a_4,$$

where

$$\begin{aligned} a_1 &= c + \frac{c}{D}, \\ a_2 &= \frac{c^2}{D} + S \left(\left(\frac{2}{B+n_2^{*2}} - \frac{\chi}{D} \right) n_2^{*2} (1-n_2^*) - 1 \right), \\ a_3 &= \frac{cS}{D} \left(\frac{2n_2^{*2}(1-n_2^*)}{B+n_2^{*2}} - 1 \right), \\ a_4 &= \frac{\chi}{D} Sn_2^*(1-n_2^*) (r + \alpha \operatorname{sech}^2(n_2^* - 1)). \end{aligned}$$

Since $n_2^* < 1$, $a_4 > 0$. If either $a_2 < 0$ and/or $a_3 < 0$ then the critical point $(n_1^*, n_2^*, 0, 0)$ is a saddle. If both $a_2 > 0$ and $a_3 > 0$ then the critical point is a stable node, i.e., if

$$\frac{c^2}{D} + S \left(\left(\frac{2}{B+n_2^{*2}} - \frac{\chi}{D} \right) n_2^{*2} (1-n_2^*) - 1 \right) > 0, \quad (39)$$

and

$$2n_2^{*2}(1-n_2^*) > B + n_2^{*2}. \quad (40)$$

From (40), we have $n_2^{*2} - 2n_2^{*3} > B > 0$. Consider the function $f(n_2^*) = n_2^{*2} - 2n_2^{*3}$ for $0 < n_2^* < 1$. Then clearly $1/27 > B > 0$. Hence, if (40) is satisfied then $c^2 > \chi S n_2^{*2} (1-n_2^*)$ is sufficient to satisfy (40).

REFERENCES

1. D. Darling and D. Tarin, The spread of cancer in the human body, *New Scientist*, 50-53 (July 1990).
2. L. Edelstein-Keshet, *Mathematical Models in Biology*, Random House, (1988).
3. M. LaBarbera and S. Vogel, The design of fluid transport systems in organisms, *American Scientist* **70**, 54-60 (1982).
4. J. Folkman, Tumor angiogenesis, *Adv. Cancer Res.* **43**, 175-203 (1985).
5. M.A. Gimbrone, R.S. Cotran, S.B. Leapman and J. Folkman, Tumor growth and neovascularization: An experimental model using the rabbit cornea, *J. Natl. Cancer Inst.* **52** (2), 413-427 (1974).
6. V.R. Muthukkaruppan, L. Kubai and R. Auerbach, Tumor-induced neovascularization in the mouse eye, *J. Natl. Cancer Inst.* **69**, 699-704 (1982).
7. M.E. Maragoudakis, P. Gullino and P.I. Lelkes, Editors, *Angiogenesis in Health and Disease*, Plenum Press, New York, (1992).
8. N. Paweletz and M. Knierim, Tumor related angiogenesis, *Crit. Rev. Oncol. Hematol.* **9**, 197-242 (1989).
9. J. Folkman and M. Klagsbrun, Angiogenic factors, *Science* **235**, 442-447 (1987).

10. D.H. Ausprunk and J. Folkman, Migration and proliferation of endothelial cells in preformed and newly formed blood vessels during tumor angiogenesis, *Microvasc. Res.* **14**, 53-65 (1977).
11. C.H. Blood and B.R. Zetter, Tumor interactions with the vasculature: Angiogenesis and tumor metastasis, *Biochem. Biophys. Acta* **1032**, 89-118 (1990).
12. J. Folkman and C. Haudenschild, Angiogenesis in vitro, *Nature* **288**, 551-556 (1980).
13. R. Langer, H. Brem, K. Falterman, M. Klein and J. Folkman, Isolation of a cartilage factor that inhibits tumor neovascularization, *Science* **193**, 70-72 (1976).
14. L.A. Liotta, G.M. Saidel and J. Kleinerman, Diffusion model of tumor vascularization and growth, *Bull. Math. Biol.* **39**, 117-128 (1977).
15. J.A. Adam and S.A. Maggelakis, Diffusion regulated growth characteristics of a spherical prevascular carcinoma, *Bull. Math. Biol.* **52** (4), 549-582 (1990).
16. H.P. Greenspan, Models for the growth of a solid tumor by diffusion, *Stud. Appl. Math* **51**, 317-340 (1972).
17. J. Denekamp, Vascular endothelium as the vulnerable element in tumours, *Acta Radiol. Oncol.* **23**, 217-225 (1984).
18. R.K. Jain, Barriers to drug delivery in solid tumors, *Sci. Am.* **271** (1), 58-65 (1994).
19. J.D. Murray, *Mathematical Biology*, Springer-Verlag, Berlin, (1989).
20. D. Balding and D.L.S. McElwain, A mathematical model of tumour induced capillary growth, *J. Theor. Biol.* **114**, 53-73 (1985).
21. J.A. Sherratt and J.D. Murray, Models of epidermal wound healing, *Proc. R. Soc. Lond. B* **241**, 29-36 (1990).
22. C.L. Stokes, D.A. Lauffenburger and S.K. Williams, Migration of individual microvessel endothelial cells: Stochastic model and parameter measurement, *J. Cell. Sci.* **99**, 419-430 (1991).
23. M.A.J. Chaplain and A.M. Stuart, A model mechanism for the chemotactic response of endothelial cells to tumour angiogenesis factor, *IMA J. Math. Appl. Med. Biol.* **10**, 149-168 (1993).
24. R.M. Shymko and L. Glass, Cellular and geometric control of tissue growth and mitotic instability, *J. Theor. Biol.* **63**, 355-374 (1976).
25. S.B. Carter, Principles of cell motility: The direction of cell movement and cancer invasion, *Nature* **208**, 1183-1187 (1965).
26. A.M. Schor and S.L. Schor, Tumour angiogenesis, *J. Pathol.* **141**, 385-413 (1983).
27. R.M. Sutherland, Cell and environment interaction in tumor microregions: The multicell spheroid model, *Science* **240**, 177-184 (1988).